

J. Whale

Post-doctoral Research Associate,
Department of Aeronautical
and Astronautical Engineering,
University of Illinois at Urbana-Champaign,
306 Talbot Laboratory,
104 South Wright Street,
Urbana, IL 61801-2935

C. J. Fisichella

Graduate Student,
Department of Mechanical
and Industrial Engineering,
University of Illinois at Urbana-Champaign,
306 Talbot Laboratory,
104 South Wright Street,
Urbana, IL 61801-2935

M. S. Selig

Associate Professor,
Department of Aeronautical
and Astronautical Engineering,
University of Illinois at Urbana-Champaign,
306 Talbot Laboratory,
104 South Wright Street,
Urbana, IL 61801-2935
e-mail: m-selig@uiuc.edu

Correcting Inflow Measurements From Wind Turbines Using a Lifting-Surface Code

In order to provide accurate blade element data for wind turbine design codes, measured three-dimensional (3D) field data must be corrected in terms of the (sectional) angle of attack. A 3D Lifting-Surface Inflow Correction Method (LSIM) has been developed with the aid of a vortex-panel code in order to calculate the relationship between measured local flow angle and angle of attack. The results show the advantages of using the 3D LSIM correction over 2D correction methods, particularly at the inboard sections of the blade where the local flow is affected by post-stall effects and the influence of the blade root. [S0199-6231(00)00604-3]

Introduction

A key parameter in aerodynamic models of horizontal-axis wind turbines (HAWTs) is the angle of attack α defined as the angle between the chord of the blade airfoil profile and the effective local velocity—the resultant of the components of axial induced and rotational velocities, where the induced velocity is that produced by the shed wake from the rotor. Measurements of force coefficients made on rotating wind turbine blades, however, are typically correlated with measurements of a local inflow angle β obtained by flow angle sensors protruding from the leading edge of the blade (see Fig. 1).

It is desirable to reduce the 3D field measurements in terms of the angle of attack α in order to provide accurate measured blade element data for comparison with 2D blade-element momentum (BEM) and dynamic stall models and other experimental results. The angle of attack is related to the inflow angle by:

$$\alpha = \beta - \alpha_n \quad (1)$$

where α_n is the angle due to the upwash induced at the local inflow point by the bound vorticity on the blade. Calculating α_n is a relatively straightforward procedure in a wind tunnel where a 2D airfoil can be positioned at a particular angle α and a probe used to measure the local inflow angle β at a point. There are significant differences, however, between 2D airfoil flow and 3D flow on a rotating blade. This is most noticeable at inboard sections of the blade where the section is experiencing stall. The Coriolis component of the 3D flow suppresses separation; delaying stall and enhancing lift at the blade section. These effects are referred to as 'stall-delay' or 'post-stall' effects [1,2].

Various methods have been proposed for calculating the relationship between α and β (and hence the 3D upwash) on a rotating blade. Madsen [3] describes a method that uses BEM to cal-

culate a HAWT power curve as a function of angle of attack at a particular spanwise position. The measured inflow angles are adjusted until good agreement is provided between the calculated and measured power curves. The inverse BEM method [4,5] assumes the measured normal and tangential forces are uniform over an annulus containing the blade section. The wake-induced velocities are calculated according to momentum theory, yielding the effective velocity vector and subsequently the angle of attack. Brand et al. [6] estimate the angle of attack using a stagnation point method. The intersection of the chord line and a line normal to the blade surface at the stagnation point yields a stagnation angle, which is used as an estimate for the angle of attack.

In order to ascertain the β - α relationship for their Combined Experiment Rotor (CER), researchers at the National Renewable Energy Laboratory (NREL) have conducted a series of 2D wind tunnel experiments [7]. A 2D scale model of the blade section was fitted with a flow sensor upstream of the section and placed in a wind tunnel. The 2D upwash obtained from these tests was used as an estimate for the 3D upwash.

The current research aims to improve on these 2D methods by calculating the flow field around a HAWT rotor using a 3D vortex-panel method. A lifting-surface code is used to model the vorticity in the wake and along the rotor blades. The 3D upwash

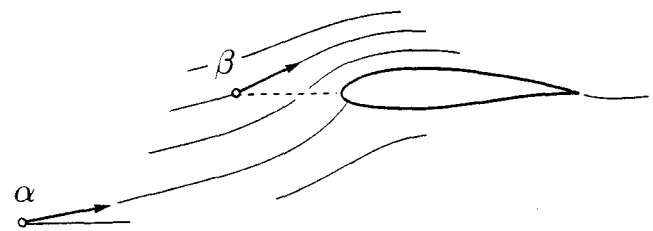


Fig. 1 Angle of attack α and local flow angle β for a blade section

Contributed by the Solar Energy Division of The American Society of Mechanical Engineers for publication in the ASME JOURNAL OF SOLAR ENERGY ENGINEERING. Manuscript received by the ASME Solar Energy Division, April 1999; final revision, September 2000. Associate Technical Editor: D. Berg.

induced by the flow field vorticity is calculated, yielding the β - α relationship at desired spanwise stations as a set of inflow correction curves. This paper shows the initial results of using the code to correct 3D data from Phase III of the CER tests conducted at NREL.

The Inflow Correction Method

An inflow correction method has been developed at the University of Illinois at Urbana-Champaign in order to provide accurate 3D corrections to HAWT aerodynamic data. The method makes use of a lifting-surface code and is referred to as the Lifting-Surface Inflow Correction Method (LSIM).

The Lifting-Surface Code. The lifting-surface code used in the method is titled 'Lifting-Surface Aerodynamics and Performance Analysis of Rotors in Axial Flight' (LSAF), developed by Kocurek [8]. The code was written for the design and analysis of helicopter rotors and extended to wind turbines. The code simulates the rotor and the wake as a lattice of vortex panels. A prescribed wake model is used which allows for roll-up of tip and root vortices, and these features were used in the current model. The detailed blade aerodynamics are computed by combining the lifting-surface model with a blade-element analysis that requires as input a table of airfoil performance characteristics. Field velocity routines in the code allow the computation of local flow angles at specified points in the flow.

Development of the Method. LSIM evolved from the consideration of the differences in 2D and 3D upwash due to post-stall effects. For inboard stations at post-stall angles of attack, the circulation around a 3D blade section is expected to be greater than that around a 2D section. As Fig. 2 illustrates, the 3D post-stall upwash is thus expected to be greater than the 2D upwash. Thus, as Fig. 3 shows, for a particular angle of attack past stall the 3D inflow angle β is higher than the 2D case (which is higher than the straight dotted line shown to represent the line of reflection $\beta = \alpha$). Consequently, for a particular inflow angle β past that of 2D stall, the 3D angle of attack α is lower than the angle predicted from the 2D correction curve. The application of the 3D correction to measured 3D lift data in Fig. 3 results in a curve that has higher lift at a given α than the curve that has been corrected with 2D data. This higher lift in turn would suggest (through a vortex lattice method and circulation considerations) greater values of inflow angle β for that particular α than specified in the 2D β - α correction curve of Fig. 3. It is this interplay between the β - α relationship and the corrected data curves that leads to the concept of an iterative inflow correction method.

The strategy behind LSIM is to use an initial estimate of the 3D β - α relationship for each spanwise station of interest and apply the inflow corrections to convert the measured raw data into airfoil performance data according to the equations:¹

$$c_l = c_n \cos \alpha + c_t \sin \alpha \quad (2)$$

$$c_{dp} = c_n \sin \alpha - c_t \cos \alpha \quad (3)$$

¹It must be noted that the convection used in Eqs. (2) and (3) is consistent with a tangential force that is defined as positive towards the leading edge of the blade.

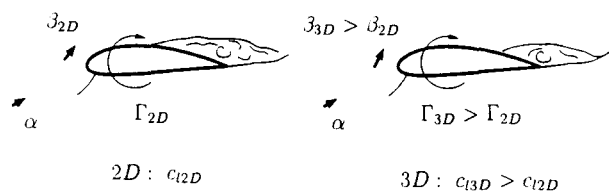


Fig. 2 Difference between 2D and 3D flow physics at a blade section

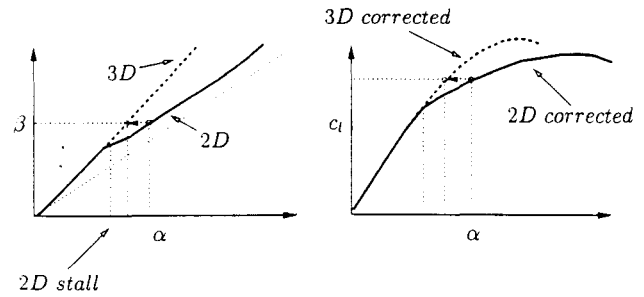


Fig. 3 Expected trends for a 3D inflow correction

where c_l and c_n are taken from measured pressure data on the blade, and hence the drag coefficient is referred to as the pressure drag coefficient.

The airfoil performance data are then input into the vortex panel code, and values of α and β are extracted at each station of interest to form new β - α relationships. The new corrections are used to correct the raw data again and the resulting performance data is input into the code once more. This procedure is repeated until converged solutions for the β - α curves are reached and a final correction can be made to the raw data. Convergence is determined by the difference in β between the current and previous iterations at each span station. When the maximum absolute value falls below a set tolerance, then the solution is assumed to have converged. A tolerance of 0.4 deg, 4-5 iterations for conver-

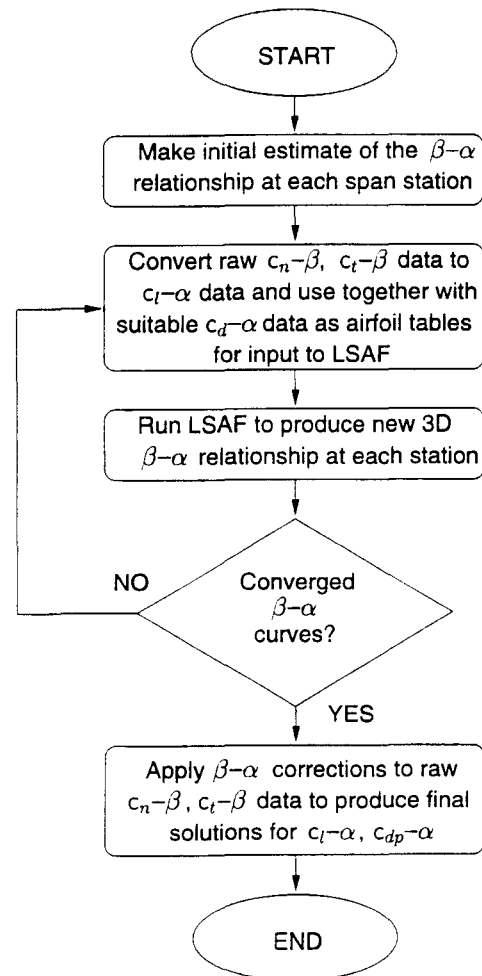


Fig. 4 Flowchart of LSIM procedure

Table 1 Operating parameters of the Phase III CER tests

Machine Operation	
Number of blades	3
Rated power	19.8 kW
Power regulation	Stall
Rotor location	Downwind
Cut-in wind speed	6 m/s
Cut-out wind speed	N/A (stall control)
Rotational speed	71.63 rpm
Density	1.025 kg/m ³
Coning angle	3.42 deg
Blade Parameters	
Type	NREL in-house
Profile	S809
Chord	0.4572 m
Thickness	0.096 m
Length	5.023 m
Tip pitch	Approx. 3 deg

gence and less than 1-min cpu time per iteration are typical. The overall procedure is outlined in Fig. 4. Additional details can be found in Whale and Selig [9,10].

Testing the Method. Testing of the correction method requires measured data that incorporates 3D flow characteristics at post-stall angles of attack. A large amount of 3D data has been gathered from the IEA Annex XIV Project: Field Rotor Aerodynamics [11] which involved the coordination of five full-scale aerodynamic test programs aimed at capturing 3D data from experiments on rotating wind turbine blades. Of these tests, the most comprehensive body of data has been gathered at NREL due to the detailed instrumentation on the CER blade.

In Phase III of the CER experiment [12], a highly twisted blade of constant chord was used. With the exception of the root, the blade has an NREL S809 profile, an airfoil that has been tested in wind tunnels at Delft University of Technology (TUDelft), Ohio State University (OSU) and Colorado State University (CSU) [7]. Table 1 shows the blade geometry and operating parameters for the CER during Phase III. Measurements of the local inflow, at a distance in front of the leading edge of the blade equal to 79% of the chord, were made with lightweight flow sensor flags for spanwise stations of 30%, 47%, 63%, and 80% of the blade radius. For the purposes of testing LSIM, it was desirable to obtain a smooth set of performance data in which irregularities in the data (e.g., due to unsteady conditions during measurement) were kept to a

minimum. A 'hypothetical' set of 3D data was produced for the CER by matching TUDelft 2D wind tunnel data and Phase III CER 3D data. Performance data from 2D wind tunnel tests on the S809 airfoil at TUDelft was input into the lifting-surface code and converted to uncorrected pre-stall data at 30%, 47%, 63%, and 80% span. Phase III CER 3D performance data was used as a guide in estimating the post-stall behavior of the hypothetical data. Plots of normal and tangential blade force coefficients versus local flow angle for the hypothetical 3D data are shown in Figs. 5(a) and 5(b), respectively.

LSIM simulations were carried out using the hypothetical data using the line of reflection as an initial inflow correction (i.e., $\alpha = \beta$ at iteration 1tn 0). In constructing the performance tables to input to the vortex code, lift values were calculated using Eq. (2) and drag values were taken from 2D TUDelft data.

Results

The inflow correction curves output from LSIM were found to converge after 4–5 iterations of the method and the results are shown in Figs. 6(a)–(d) for the 30%, 47%, 63%, and 80% span stations, respectively. In each case, the 3D curves are compared with 2D inflow correction curves (i.e., using 2D TUDelft lift and drag values as input to LSIM).

At 30% span, there is a significant departure in the post-stall β - α relationship between the 2D and 3D correction methods. Figure 6(a) shows $\beta_{3D} > \beta_{2D}$ for some post-stall α , as expected from the theory outlined in Fig. 2. In particular, at $\beta = 20$ deg there is a difference of around 4 deg between applying a 2D LSIM or a 3D LSIM correction to the raw measurement data. At the 47% and 63% span stations, the deviation between the 2D and 3D curves is less significant with a difference of less than 0.5 deg between applying a 2D or a 3D correction across the range of raw β values. Further outboard, at 80% span, the differences between the 2D and 3D curves are negligible.

The converged 3D inflow correction curves were linearly extrapolated to higher angles of attack over the entire β range of the hypothetical input data and extended trendlines were used to apply the 3D LSIM corrections to the data at each spanwise location, and produce values of lift and pressure drag in accordance with Eqs. (2) and (3). The errors introduced by extending the inflow correction curves are discussed before the conclusions of this paper. From the equations it can be seen that applying the inflow correction will affect both the general slope and intercept of the 3D performance curves. The 3D corrected lift and pressure drag curves produced by LSIM are shown in Fig. 7, together with corresponding 2D data from wind tunnel tests at TUDelft ($Re = 500,000$).

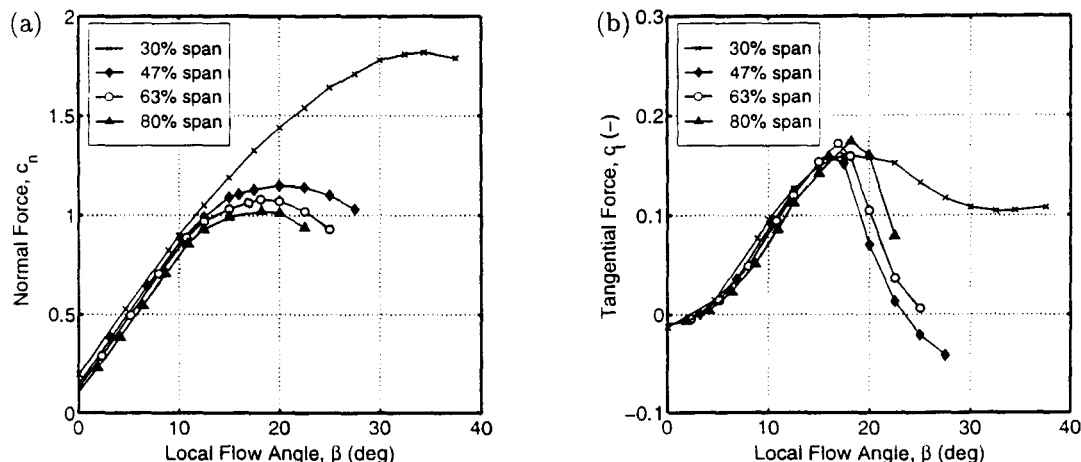


Fig. 5 Hypothetical performance data based on Phase III CER values: (a) Normal force, (b) Tangential force

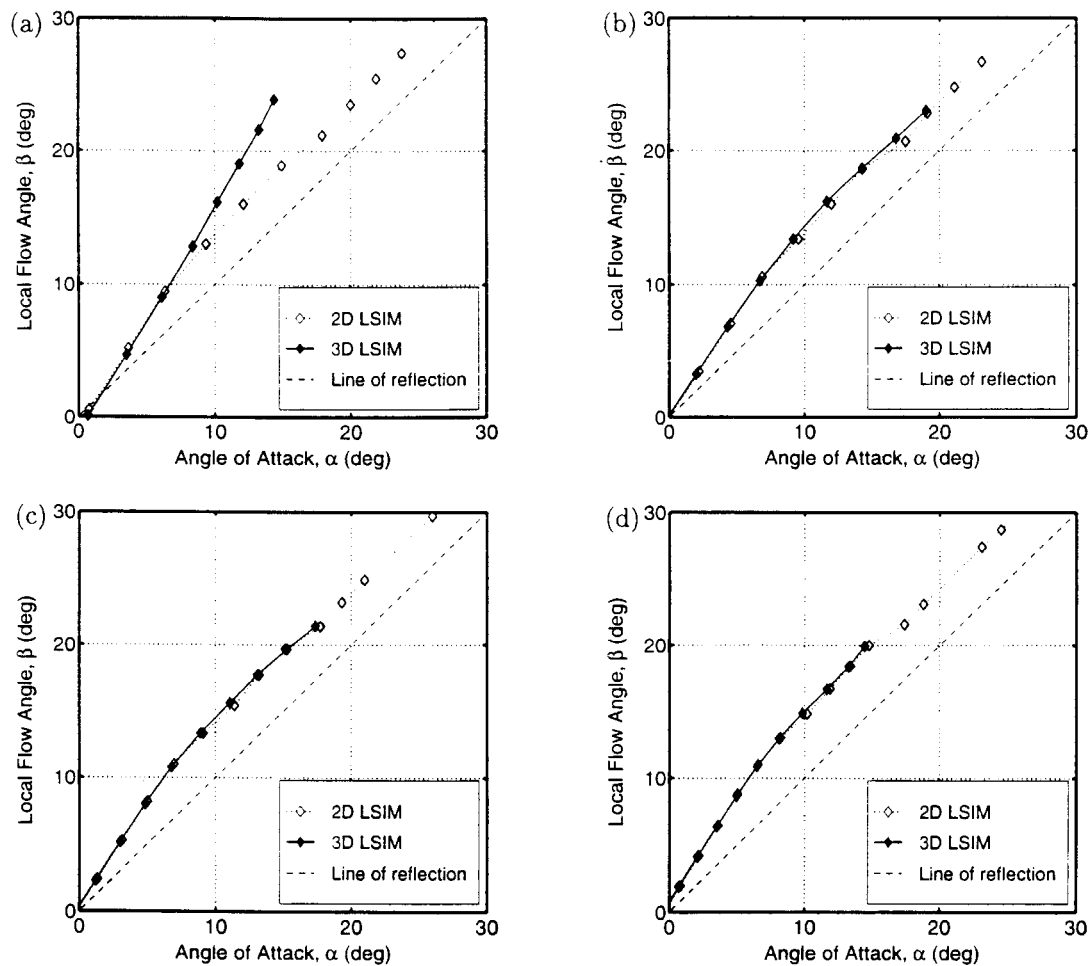


Fig. 6 LSIM inflow correction curves for CER hypothetical lift data: (a) 30% span, (b) 47% span, (c) 68% span, (d) 98% span

At the 30% station (Fig. 7(a)), there is a marked enhancement of the 3D lift as compared with the 2D data. The increase in lift is as much as 75% at some angles of attack and the converged LSIM curve shows an 11-degree delay in stall compared with the 2D data. Figures 7(b)–(d) show that the differences between the 2D wind-tunnel lift data and the 3D predictions decrease significantly with spanwise location up to 80% span. In particular, there is good correlation with 2D data at 63% and 80% span, suggesting the upwash at these stations is too far outboard to be significantly influenced by post-stall effects and too far inboard to be affected by the tip vortex.

Comparing the 2D wind-tunnel drag data with the 3D converged solutions in Fig. 7, there is a significant increase in 3D pressure drag over 2D values at 30% span and at some angles of attack, the increase in drag is as much as 120%. This seems contrary to the theory of post-stall suppressed wake-enhanced lift (outlined in Fig. 2 and used by many researchers in modeling post-stall effects, e.g., Montgomerie [1], Du and Selig [13]). The phenomenon of greater 3D drag at inboard stations than 2D drag, however, has also been observed in experiments by Madsen [3] and Björck et al. [14] and warrants further investigation. Figures 7(b)–(d) show the discrepancies between 3D calculations of pressure drag and 2D data reduce with spanwise location up to 80% span. In particular, there is a very good agreement between 2D and 3D values at 80% span, highlighting the 2D nature of the flow at this span station.

Comparison with 2D Methods. In order to compare the new 3D method with 2D methods, the converged 3D LSIM perfor-

mance curves of Fig. 7 were compared with a 2D LSIM correction method, i.e., using 2D TUDelft lift and drag values as input to the lifting-surface code. In addition, results are also shown from a 2D wind tunnel method (WTM) developed from 2D upwash trends established in OSU/CSU wind tunnel tests and currently used as a correction method at NREL. The equation for the 2D correction derived from the wind-tunnel tests is shown in Eq. (4):

$$\alpha = -5.427 \times 10^{-5} \beta^3 + 6.713 \times 10^{-3} \beta^2 + 0.617 \beta - 0.8293 \quad (4)$$

Figures 8(a)–(d) show the comparison of corrected lift and pressure drag data at each spanwise station. At 30% span, the 3D LSIM predicts greater post-stall lift and pressure drag than the 2D LSIM. The graph shows differences of as much as 15% in c_l and 35% in c_{dp} between applying a 2D or a 3D correction. For the 47% station (and stations further outboard), the difference between applying a 2D or 3D correction is less than 0.1% and can be regarded as negligible.

Comparisons of the 3D LSIM and 2D WTM curves show lower LSIM lift values for pre-stall angles of attack and higher LSIM lift values for post-stall angles of attack. This trend is most evident at 30% span (Fig. 8(a)) and may be explained by considering the associated behavior in upwash. At pre-stall angles of attack, the trend in lift suggests a lower LSIM upwash than the 2D upwash of the wind tunnel method and is likely to be due to the influence of the 3D geometry at the root of the blade. At post-stall angles of attack, 3D LSIM predicts greater upwash than the 2D WTM up-

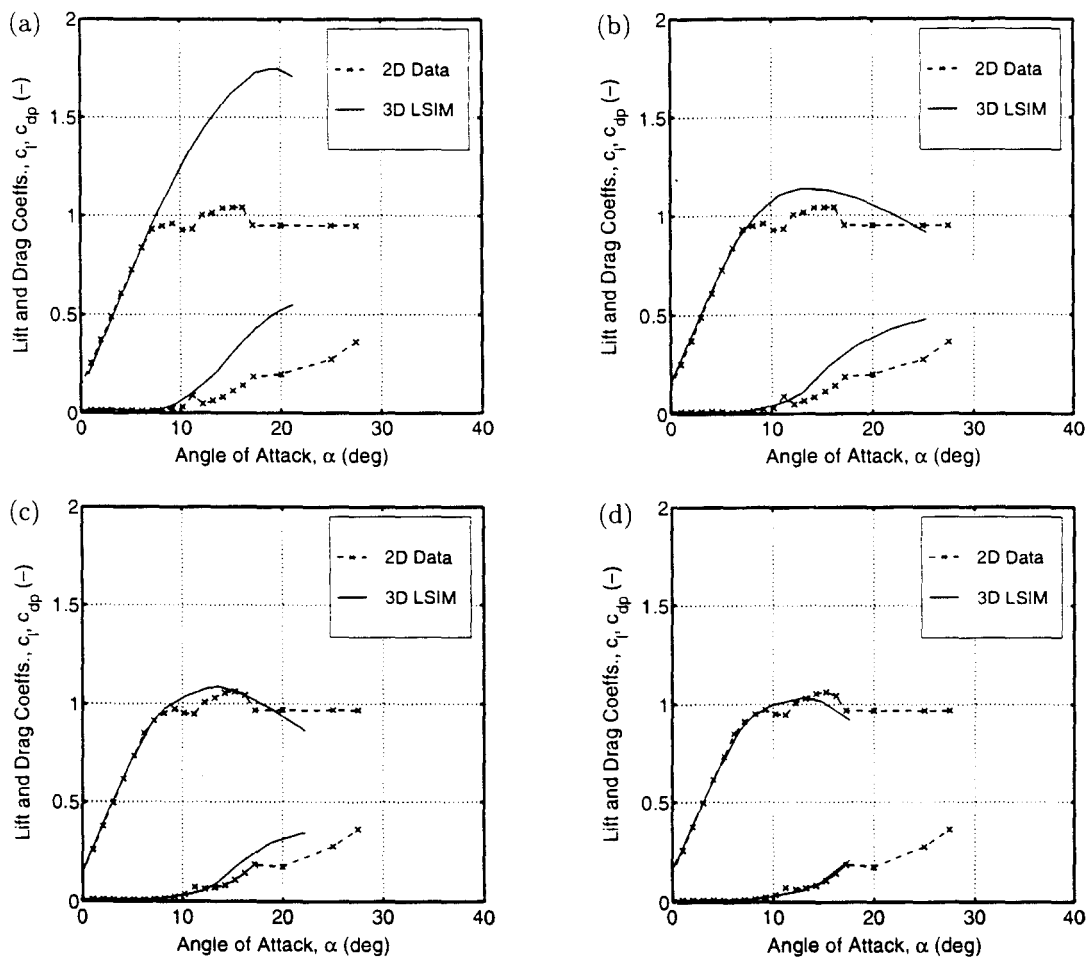


Fig. 7 LSIM corrected performance curves for CER hypothetical lift data: (a) 30% span, (b) 47% span, (c) 68% span, (d) 98% span

wash due to the 3D effects outlined in Fig. 2. In terms of pressure drag, the 3D model predicts high values at 30% span that appear to be associated with high post-stall lift (as discussed previously). Figures 8(a)–(d) show, as spanwise station increases, there is improved agreement between the LSIM and WTM curves due to the 2D nature of the flow at the outboard stations.

Finally, it should be noted that these trends may differ in the case of comparing 2D and 3D data for a different turbine since the current LSIM correction takes into account the particular geometry and upwash of the CER blade.

Discussion of Errors

Application of the correction method shows that the range of calculated α values, corresponding to the range of raw β values, reduces with each iteration. Figure 9(a) gives an example of the trend in the β – α relationship after 4 iterations of LSIM. The curves are similar to those produced at 30% span using the hypothetical input data. Initially the range of α equals the range of β since our first estimate (ltn 0) of the relationship is $\beta = \alpha$. In subsequent iterations, Fig. 9(a) shows that for a set β value, successively smaller values of α are generated. Thus, the vortex-panel code is run with successively smaller ranges of α (Fig. 9(b)) and the range of values over which the β – α relationship is known reduces with each iteration introducing the need for extrapolation. In the above work, trendlines were used to extend the β – α relationship over the entire range of raw β values, introducing errors in the correction of the raw data at the higher β values. A possible solution to this ‘angle-range reduction’ problem is to acquire ex-

perimental data over a large β range which, despite undergoing reduction in LSIM, will still produce values for the β – α relationship over a suitably large range of α .

Conclusions

A 3D Lifting-Surface Inflow Correction Method (LSIM) has been developed with the aid of a vortex-panel code in order to calculate inflow correction curves (the relationship between the angle of attack and the local flow angle measured on the HAWT). The method has been tested using hypothetical 3D input data, based on 3D measurements from the Combined Experiment Rotor (CER) at the National Renewable Energy Laboratory and 2D wind tunnel tests at Delft University of Technology. The method, tested at each of four spanwise stations (30%, 47%, 63%, and 80%), was shown to successfully produce converged solutions for the inflow correction curves. The method has given insight into 3D post-stall behavior at inboard blade stations, highlighting the enhanced lift and showing increased pressure drag compared with 2D wind tunnel data. The latter phenomenon, consistent with measurements made at The Aeronautical Research Institute of Sweden and Risø National Laboratory, Denmark, requires further investigation into the detailed flow physics.

Comparison of the new method with 2D methods suggests that, due to the 3D geometry at the root and 3D flow effects at inboard stations, the 2D wind tunnel method of correction currently in use at NREL overpredicts the upwash at pre-stall angles of attack and underpredicts upwash at post-stall angles of attack. In addition, the method has shown significant differences between a 3D cor-

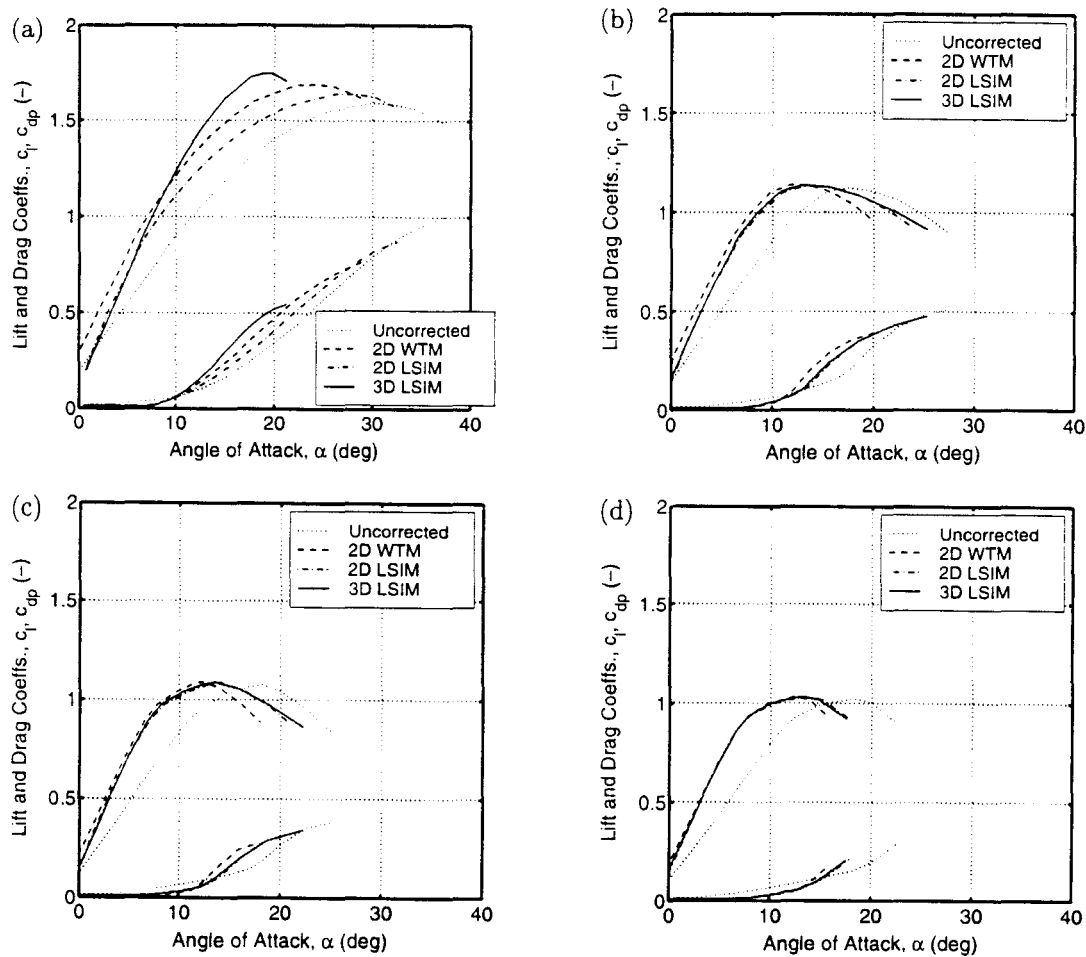


Fig. 8 Comparison of 3D LSIM with 2D methods: (a) 30% span, (b) 47% span, (c) 63% span, (d) 80% span

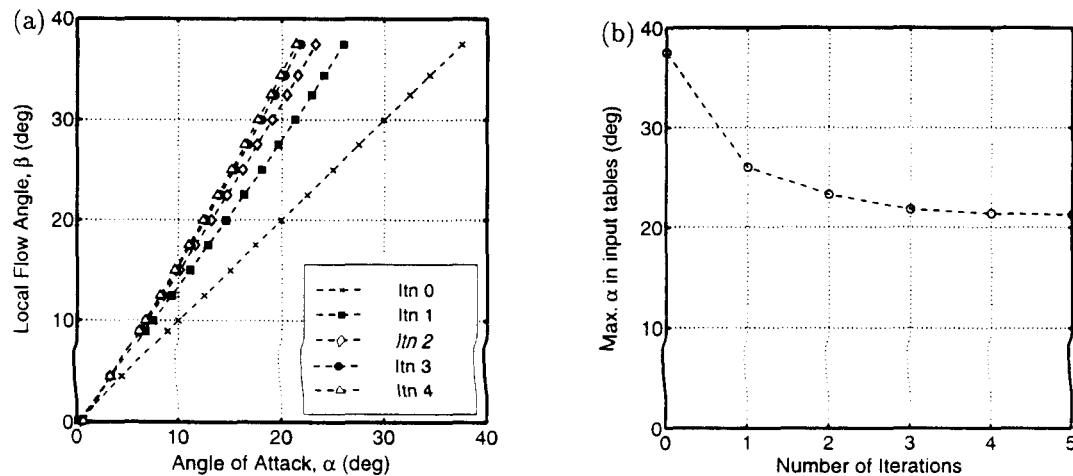


Fig. 9 Illustration of the LSIM angle-range reduction problem: (a) Trends in $\beta-\alpha$, (b) Range of α input to LSIM

rection and a 2D correction at the innermost station of 30% span, particularly at high angles of attack (where accurate performance data is essential for peak power prediction). Further outboard, this study has shown that in the case of the CER data, sufficient accuracy may be obtained using the method together with 2D performance data and may indicate that 3D flow effects do not persist more than halfway along the blade span.

In conclusion, LSIM recognizes the important differences between 2D and 3D flows on a wind turbine blade section and appears to be a very promising method of producing accurate corrections of HAWT measurements. Further evaluation of the method awaits 3D data recorded under steady-state operating conditions and the planned CER tests in the NASA Ames wind tunnel may provide this opportunity.

Acknowledgments

This work was undertaken with the support of the National Renewable Energy Laboratory under Subcontract No. XCX-7-16466-01 (Technical Monitor: J. L. Tangler). The assistance of M. M. Hand of NREL in preparing the raw CER data is gratefully acknowledged. In addition, the authors would like to thank J. D. Kocurek for providing the LSAF code that was used in determining the 3D rotor flow.

Nomenclature

- a = Axial induction factor
 c_n = Coefficient of normal force
 c_t = Coefficient of tangential force
 c_l = Coefficient of lift
 c_d = Coefficient of drag
 c_{dmin} = Minimum value of drag coefficient
 c_{dp} = Coefficient of pressure
 Re = Reynolds number

Greek Symbols

- α = Sectional angle of attack
 α_u = Angle due to upwash at local inflow point
 β = Measured local flow angle
 Γ = Circulation around blade section

References

- [1] Montgomerie, B., 1994, "The Influence of 3D Effects in Lift and Drag on the Performance of a Stalled Horizontal Axis Wind Turbine Rotor," *Proceedings, 8th IEA Symposiums on Aerodynamics of Wind Turbines*, Lyngby, Denmark, pp. 101–107.
- [2] Wood, D. H., 1991, "A Three Dimensional Analysis of Stall Delay on a Horizontal Axis Wind Turbine," *J. Wind Eng. Ind. Aero.*, **37**, pp. 1–14.
- [3] Madsen, H. A., 1991, "Aerodynamics of a Horizontal-Axis Wind Turbine in Natural Conditions," *Risø Report M-2903*, Risø National Laboratory, Roskilde, Denmark.
- [4] Bruining, A., and van Rooij, R.P.J.O.M., 1997, "Two- and Three-Dimensional Aerodynamic Performance of the NLF(1)-0416 Airfoil on a Wind Turbine Blade," *Proceedings, 11th IEA Symposium on Aerodynamics of Wind Turbines*, Petten, Netherlands, pp. 59–76.
- [5] Snel, H., Houwink, R., Bosschers, J., Piers, W. J., van Bussel, G., and Bruining, A., 1993, "Sectional Prediction of 3-D Effects For Stalled Flow on Rotating Blades and Comparison with Measurements," *Proceedings, 1993 European Community Wind Energy Conference*, Travemünde, Germany, pp. 395–399.
- [6] Brand, A. J., Dekker, J. W. M., de Groot, C. M., and Späth, M., 1997, "Field Rotor Aerodynamics: The Rotating Case," *Proceedings, 16th ASME Wind Energy Symposium*, Reno, NV, pp. 319–327.
- [7] Butterfield, C. P., Musial, W. P., and Simms, D. A., 1992, "Combined Experimental Phase I, Final Report," NREL Report TP-257-4655, National Renewable Energy Laboratories, Golden, CO.
- [8] Kocurek, D., 1987, "Lifting Surface Performance Analysis for Horizontal Axis Wind Turbines," NREL Subcontract Report STR-217-3163, National Renewable Energy Laboratories, Golden, CO.
- [9] Whale, J., and Selig, M. S., 1999, "Lifting-Surface Inflow Correction Method (LSIM), User's Manual," University of Illinois at Urbana-Champaign, Dept. of Aeronautical and Astronautical Engineering, AAE 99-11, UILU ENG 99-05-11, Urbana, IL.
- [10] Whale, J., and Selig, M. S., 1999, "LSIM: A Lifting-Surface Inflow Correction Method," University of Illinois at Urbana-Champaign, Dept. of Aeronautical and Astronautical Engineering, AAE 99-12, UILU ENG 99-05-12, Urbana, IL.
- [11] Schepers, J. G., 1997, "Final Report of IEA Annex XIV: Field Rotor Aerodynamics," ECN Report ECN-C-97-027, Netherlands Energy Research Foundation, Petten, Netherlands.
- [12] Simms, D. A., Robinson, M. S., Hand, M. M., and Fingersh, L. J., 1996, "Characterization and Comparison of Baseline Aerodynamic Performance of Optimally-Twisted versus Non-Twisted Blades," *1996 Proceedings, ASME Energy-Source Technology Conference*, Houston, TX, pp. 143–148.
- [13] Du, Z., and Selig, M. S., 1998, "3-D Stall-Delay Model for Horizontal Axis Wind Turbine Performance Prediction," *Proceedings, 17th ASME Wind Energy Symposium*, Reno, NV, pp. 9–19.
- [14] Björck, A., Ronsten, G., and Montgomerie, B., 1995, "Aerodynamic Section Characteristics of a Rotating and Non-rotating 2.375m Wind Turbine Blade," FFA Report TN 1995-03, The Aeronautical Research Institute of Sweden, Bromma, Sweden.